Free-vibration tailoring of single- and multi-bay laminated box structures by refined beam theories

Free-vibration tailoring of single- and multi-bay laminated box structures by refined beam theories

E. Carrera[a]*, M. Filippi[a]†, P. K. Mahato[b]‡, A. Pagani[a]§
[a]Department of Mechanical and Aerospace Engineering, Politecnico di Torino,
Corso Duca degli Abruzzi 24, 10129 Torino, Italy.
[b]Department of Mechanical Engineering,
Indian School of Mines, Dhanbad-826004, India.

Submitted to:

Thin-Walled Structures

*Professor of Aerospace Structures and Aeroelasticity, e-mail: erasmo.carrera@polito.it
†Research Fellow, e-mail: matteo.filippi@polito.it
‡Assistant Professor, e-mail: mahato.pk.mech@ismdhanbad.ac.in
§Research Fellow, e-mail:alfonso.pagani@polito.it

Abstract

By employing refined beam theories, free vibration analysis and tailoring of laminated composite box structures are discussed in this work. Higher-order models are implemented utilizing the Carrera Unified Formulation (CUF), according to which the mechanical variables are expressed in terms of arbitrary expansion of the generalized unknowns. The proposed 1D models have only pure displacement variables, are geometrically consistent and have component-wise capabilities because Lagrange polynomials are used in the framework of CUF to formulate refined kinematics theories. Moreover, since the finite element method is used to interpolate the generalized unknowns, arbitrary anisotropy, geometry and boundary/loading conditions can be considered with no loss of generality. The resulting methodology is exploited to analyze single- and multi-bay composite laminated box beams for aerospace applications. Particular emphasis is given to the parametric study and tailoring of the lamination scheme versus free vibration characteristics for various box structures. Also, the effects of cut-offs are investigated. The numerical results are compared to those from the literature and commercial finite element software tools. The study widely demonstrates the high computational efficiency and the refined capabilities of the proposed CUF-based models, which can be considered as ideal candidates for the detailed tailoring of aerospace composite structures and, possibly, for future implementation into an optimization procedure.

Keywords: Laminated box beams; Composite beams; Free vibration analysis; Tailoring; Carrera Unified Formulation.

1 Introduction

In modern times, laminated composite beams, plate, and shells are extensively used in various weight-sensitive structures like high-speed aircraft, rockets, and launch vehicles because of their high specific strength and stiffness. Also, the directional properties of this class of composite materials represent a significant advantage and allow the analysts to *tailor*, eventually, the mechanical characteristics of structures given the design requirements and loading conditions.

Starting from the past centuries, many researchers have worked on the development of theories able to model the mechanical behaviour and the rheological characteristics of laminated composite structures accurately. It is clear that the classical theories of Kirchhoff (for plates) and Euler-Bernoulli (for beams) are inadequate for the modelling the composite structures. Modern models for composite structures can be divided into two main macro-categories: Equivalent Single Layer (ESL) and Layer-Wise (LW) theories. In ESL theories, the number of unknowns is independent of the number of layers: many eminent works fall into this category, and some of them are briefly discussed in the following. First- and second-order shear deformation theories (see for example [1] and [2], respectively) emerged out with improved results if compared to classical models. Third-order shear deformation theories, which satisfy the homogeneous condition of the shear stress at the unloaded boundaries, were also proposed for the analysis of beams [3] and plates [4]. Recently, a new inverse hyperbolic zig-zag shear deformation theory was studied by Sahoo and Singh [5] for static analysis of sandwich laminated plates. In this work, the authors represented their refined distribution of in-plane displacement along the thickness and compared it to the third-order polynomial expansions from conventional theories. Carrera [6] compared different 2D theories in order to investigate the effects of the curvature and the shear deformation on the buckling and vibrations of cross-ply laminated shells. Shi and Lam [7] carried out free vibration analysis of composite beams using higher order theory and assuming the odd power of the z-coordinate for the axial displacement. The mixed finite element (FE) formulation was utilized by the Ozutok et al. [8] for the free vibration analysis of the cross-ply laminated beam, whereas Rao et. al. [9] applied mixed formulation through the thickness continuity of transverse stress and displacement field. Banerjee et al. [10] used the dynamic stiffness method for the vibration analysis of the composite beams for the application to aircraft wings.

ESL results in efficient theories of structures for laminates. However, the main drawback of this approach is that the continuity of transverse shear and normal stresses is not always assured. In models based on LW approach, the number of degrees of freedom (from now on DOFs) depends directly on the number of layers. LW represents a more accurate representation of the reality, although it is generally more expensive than ESL concerning computational costs. One of the earlier attempts to describe composite laminates by LW approach can be attributed to Lekhnitskii [11], who proposed plane-stress models to reproduce piecewise continuous displacement and transverse stress fields in the thickness direction of composite plates and beams in his book. Robin and Reddy [12] used the LW laminate theory to develop

a layer-wise displacement-based FE model for laminated composite plates. Shimpi and Ainapure [13] presented an LW trigonometric shear deformation theory based on FE method for beam structures. Dinghe et al. [14] proposed a static analysis of LW/solid element method for sandwich plates structures. Kapuria et al. [15, 16] used refined hybrid theory and third-order zig-zag plate theory for through-the-thickness representation of structural deformation and electrical potential.

The main aim of the present paper is to propose an efficient and still effective structural model for the free vibration analysis and composite tailoring [17] of structures for aerospace applications, such as box beams including cut-offs and reinforcements. Considerable work for the modelling of metallic homogeneous box structures was carried out by Vlasov [18]. Composite box beams, on the other hand, present anisotropic behavior which results in different types of structural coupling, such as extension-twisting, extension-bending, etc. Due to the complex anisotropy and mechanical response composite box structures are affected by, 3D-like structural models are commonly employed , see for example [19, 20]. Nevertheless, 3D models are computationally costly, and many researchers attempted to develop simple and efficient 1D beam theories for the analysis of this kind of constructions. Kim and White [21, 22] developed a 3D-like laminated box beam model of arbitrary cross-sections beam. The primary and secondary torsional warping and transverse shear effects were included for the analysis of thin- and thick-wall beams with close cross-section. Dancila and Armanios [23] studied the effect of couplings. Volvoi et. al. [24, 25] also assessed different box beam models. Yu et. al. [26] formulated a generalized beam model (based on a Timoshenko-like formulation) for the analysis of initially curved and twisted, thin- and thick-walled anisotropic composite beams. In this work, the classical and non-classical couplings were included based on the VAM (Variational Asymptotic Method). The same authors [27] developed a generalized model for anisotropic composite box structures based on the Vlasov theory. Wu et. al [28] presented the initial-value solutions of static equilibrium differential equations of single-cell, thin-walled composite-laminated box beams under bending loads with consideration of both shear lag and shear deformation. Vo and Lee [29, 30] developed an analytical model of thin-walled composite box beams. This model was based on the first-order shear-deformable beam theory and accounted for all the structural couplings coming from the material anisotropy. Qin and Librescu [31] considered the transverse shear and the nonuniformity of membrane shear as well as the primary and secondary warping. The static and dynamic analyses of CUS (Circumferentially Uniform Stiffness) and CAS (Circumferentially Asymmetric Stiffness) beam were analysed in [31]. Shadmehri et al. [32] incorporated material anisotropy, transverse shear, warping inhibition, nonuniform torsional model, and rotary inertia for the analysis of CAS box beams. Also, Friedmann et al. [33] examined the compatibility between the FE cross-sectional analysis method based on VABS (Variational Asymptotic Beam Section Analysis) and a helicopter rotor blade model which is part of a comprehensive rotorcraft analysis code. This research resulted in an improved model able to take into account arbitrary cross-sectional warping, in-plane stresses, and moderate deflections.

Recently, beam elements for the analysis of composite box beams were also developed by Mitra et. al. [34] and Sheikh and Sheikh and Thomsen [35]. The latter work, particularly, described a model able to analyse both closed and open cross-section composite box structures.

In this paper, an advanced 1D model for the analysis of composite box structures with cut-off and transverse reinforcements is proposed. Particular emphasis is given to the vibration tailoring of the lamination sequences, which is an important topic in modern industrial applications. The devised model is based on the Carrera Unified Formulation (CUF), which allows one to implement theories of structures in an automatic manner by expressing the generalized mechanical variables in terms of generic expansion on the beam cross-section. Although CUF was initially developed for plate and shell structures [36, 37], it has been employed extensively during the last decade for the development of beam theories [38]. In this paper, in particular, Lagrange Expansion (LE) CUF beam models are employed, because of their capabilities to readily deal with arbitrary material anisotropy and complex geometries in a component-wise scenario, see for example [39, 40, 41, 42, 43, 44]. The paper is organized as follows: (i) First, preliminary considerations about elasticity and CUF are briefly discussed; (ii) The FE formulation of LE models are, then, proposed in Section 2.3; (iii) Numerical results and comparison with solutions from the literature and commercial FE codes are subsequently proposed in Section 3; (iv) The main conclusions are finally remarked in the concluding section.

2 Unified formulation

2.1 Preliminaries

The adopted coordinate frame is presented in Fig. 1, together with a generic beam geometry. The beam boundaries over y are $0 \leq y \leq L$, whereas the cross-section is denoted to as Ω. The three-dimensional displacement vector is

$$\mathbf{u}(x,y,z) = \left\{ \begin{array}{ccc} u_x & u_y & u_z \end{array} \right\}^T \tag{1}$$

For the sake of simplicity, the stress ($\boldsymbol{\sigma}$) and strain ($\boldsymbol{\epsilon}$) components are grouped as follows:

$$\begin{array}{ll} \boldsymbol{\sigma}_p = \left\{ \begin{array}{ccc} \sigma_{zz} & \sigma_{xx} & \sigma_{zx} \end{array} \right\}^T, & \boldsymbol{\epsilon}_p = \left\{ \begin{array}{ccc} \epsilon_{zz} & \epsilon_{xx} & \epsilon_{zx} \end{array} \right\}^T \\ \boldsymbol{\sigma}_n = \left\{ \begin{array}{ccc} \sigma_{zy} & \sigma_{xy} & \sigma_{yy} \end{array} \right\}^T, & \boldsymbol{\epsilon}_n = \left\{ \begin{array}{ccc} \epsilon_{zy} & \epsilon_{xy} & \epsilon_{yy} \end{array} \right\}^T \end{array} \tag{2}$$

The subscript "n" stands for terms lying on the cross-section, while "p" stands for terms lying on planes which are orthogonal to Ω. The displacement and strain components are related each other by means of

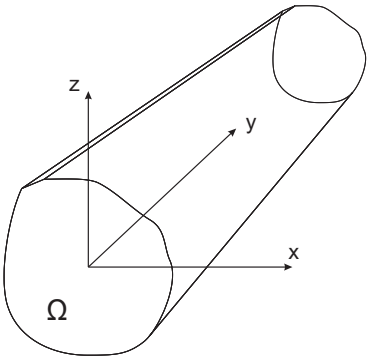

Figure 1: Coordinate frame of the beam model.

linear relationships, which are given in the following:

$$\begin{aligned} \boldsymbol{\epsilon}_p &= \boldsymbol{D}_p \mathbf{u} \\ \boldsymbol{\epsilon}_n &= \boldsymbol{D}_n \mathbf{u} = (\boldsymbol{D}_{n\Omega} + \boldsymbol{D}_{ny})\mathbf{u} \end{aligned} \tag{3}$$

where:

$$\boldsymbol{D}_p = \begin{bmatrix} 0 & 0 & \frac{\partial}{\partial z} \\ \frac{\partial}{\partial x} & 0 & 0 \\ \frac{\partial}{\partial z} & 0 & \frac{\partial}{\partial x} \end{bmatrix}, \quad \boldsymbol{D}_{n\Omega} = \begin{bmatrix} 0 & \frac{\partial}{\partial z} & 0 \\ 0 & \frac{\partial}{\partial x} & 0 \\ 0 & 0 & 0 \end{bmatrix}, \quad \boldsymbol{D}_{ny} = \begin{bmatrix} 0 & 0 & \frac{\partial}{\partial y} \\ \frac{\partial}{\partial y} & 0 & 0 \\ 0 & \frac{\partial}{\partial y} & 0 \end{bmatrix} \tag{4}$$

The Hooke law is used to express stress-strain dependency as follows:

$$\boldsymbol{\sigma} = \tilde{\boldsymbol{C}}\boldsymbol{\epsilon} \tag{5}$$

According to Eq. (2), Eq. (5) becomes:

$$\begin{aligned} \boldsymbol{\sigma}_p &= \tilde{\boldsymbol{C}}_{pp}\boldsymbol{\epsilon}_p + \tilde{\boldsymbol{C}}_{pn}\boldsymbol{\epsilon}_n \\ \boldsymbol{\sigma}_n &= \tilde{\boldsymbol{C}}_{np}\boldsymbol{\epsilon}_p + \tilde{\boldsymbol{C}}_{nn}\boldsymbol{\epsilon}_n \end{aligned} \tag{6}$$

In this paper, particular attention is given to composite box structures. Box beams can be considered as constituted by a certain number of walls made of anisotropic material. Each wall of the box is made of a combination of orthotropic fibre-composite layers whose material coordinate system $(1, 2, 3)$ generally do not coincide with the physical coordinate system (x, y, z), see Fig. 2. With respect to the global reference system, the single layer of the composite box structure is anisotropic, thus, the matrices containing the material coefficients are fully populated:

$$\tilde{\boldsymbol{C}}_{pp} = \begin{bmatrix} \tilde{C}_{11} & \tilde{C}_{12} & \tilde{C}_{14} \\ \tilde{C}_{12} & \tilde{C}_{22} & \tilde{C}_{24} \\ \tilde{C}_{14} & \tilde{C}_{24} & \tilde{C}_{44} \end{bmatrix}, \quad \tilde{\boldsymbol{C}}_{pn} = \begin{bmatrix} \tilde{C}_{15} & \tilde{C}_{16} & \tilde{C}_{13} \\ \tilde{C}_{25} & \tilde{C}_{26} & \tilde{C}_{23} \\ \tilde{C}_{45} & \tilde{C}_{46} & \tilde{C}_{43} \end{bmatrix}, \quad \tilde{\boldsymbol{C}}_{nn} = \begin{bmatrix} \tilde{C}_{55} & \tilde{C}_{56} & \tilde{C}_{35} \\ \tilde{C}_{56} & \tilde{C}_{66} & \tilde{C}_{36} \\ \tilde{C}_{35} & \tilde{C}_{36} & \tilde{C}_{33} \end{bmatrix} \tag{7}$$

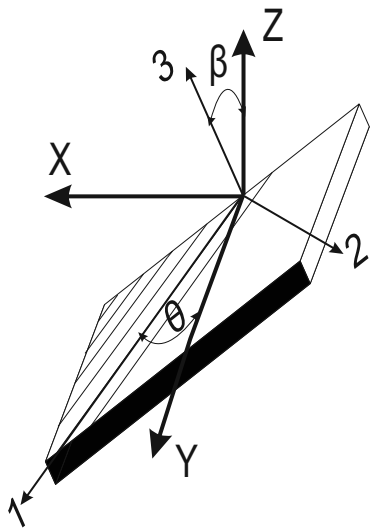

Figure 2: Physical and material reference systems.

The explicit forms of the coefficients of the matrices $\tilde{\boldsymbol{C}}_{ij}$ are not here reported for the sake of brevity, but they can be found in [45] as functions of the rotations of the fibres both in xy- and xz-planes.

2.2 Refined LE beam theories

Within the framework of CUF, the three-dimensional displacement field is the expansion of generic cross-sectional functions, F_τ

$$\boldsymbol{u}(x,y,z) = F_\tau(x,z)\boldsymbol{u}_\tau(y) \qquad \tau = 1,2,\ldots,M \tag{8}$$

where $\boldsymbol{u}_\tau$ is the vector of the *generalized* displacements, M is the number of terms of the expansion and τ indicates summation. Depending on the choice of F_τ functions, beam theories with different kinematics and approximation order can be straightforwardly implemented. In this work, 1D CUF models are implemented by means of LE (Lagrange Expansion), which utilizes Lagrange polynomial expansions of the primary mechanical variables for the development of refined kinematics beam theories. For example, a bi-quadratic beam theory can be developed by employing a nine-point (L9) Lagrange polynomial set as F_τ cross-sectional functions. For the sake of clearness, the L9 polynomials are given in the following:

$$F_\tau = \tfrac{1}{4}(r^2 + r\ r_\tau)(s^2 + s\ s_\tau) \qquad \tau = 1,3,5,7$$

$$F_\tau = \tfrac{1}{2}s_\tau^2(s^2 - s\ s_\tau)(1-r^2) + \tfrac{1}{2}r_\tau^2(r^2 - r\ r_\tau)(1-s^2) \qquad \tau = 2,4,6,8 \tag{9}$$

$$F_\tau = (1-r^2)(1-s^2) \qquad \tau = 9$$

where r and s vary from -1 to $+1$, whereas r_τ and s_τ are the coordinates of the nine zeroes of the L9 and whose locations in the natural coordinate frame are graphically shown in Fig. 3. The refined beam

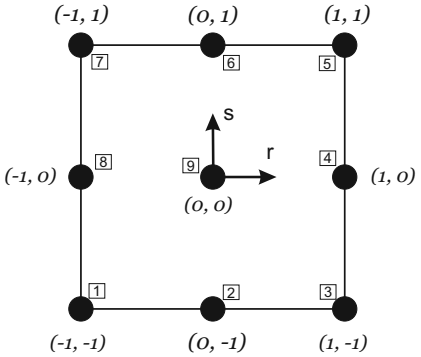

Figure 3: Natural coordinate system and zeroes of the L9 polynomial set.

model given by the use of one single L9 polynomial set for the approximation of the kinematics is

$$\begin{aligned} u_x &= F_1\, u_{x_1} + F_2\, u_{x_2} + F_3\, u_{x_3} + ... + F_9\, u_{x_9} \\ u_y &= F_1\, u_{y_1} + F_2\, u_{y_2} + F_3\, u_{y_3} + ... + F_9\, u_{y_9} \\ u_z &= F_1\, u_{z_1} + F_2\, u_{z_2} + F_3\, u_{z_3} + ... + F_9\, u_{z_9} \end{aligned} \tag{10}$$

where $u_{x_1}, ..., u_{z_9}$ are the displacement variables of the problem and they represent the translational displacement components at the L9 zeroes. In fact, refined LE models make use of only displacement variables.

The kinematics of LE beam models can be further enhanced by using higher-order Lagrange polynomials or, eventually, by adopting a combination of Lagrange polynomials on the cross-section domain Ω. The latter, also allows one to deal with complex geometries (see [46]) and to develop physically consistent refined models in a component-wise scenario [42, 41, 43, 44].

2.3 Finite element formulation

The finite element approach is adopted to discretize the structure along the y-axis. Thus, the generalized displacements $\boldsymbol{u}_\tau(y)$ are approximated as follows:

$$\boldsymbol{u}_\tau(y) = N_i(y)\mathbf{q}_{\tau i} \qquad i = 1, 2, \ldots, p+1 \tag{11}$$

where N_i stands for the i-th shape function, p is the order of the shape functions, and i indicates summation. $\mathbf{q}_{\tau i}$ is the following vector of the FE nodal parameters:

$$\mathbf{q}_{\tau i} = \left\{ \begin{array}{ccc} q_{u_{x_{\tau i}}} & q_{u_{y_{\tau i}}} & q_{u_{z_{\tau i}}} \end{array} \right\}^T \tag{12}$$

For the sake of brevity, the shape functions N_i are not reported here. They can be found in many reference texts, for instance in [47]. However, it should be underlined that the choice of the cross-section

polynomials sets for the LE kinematics (i.e. the choice of the type, the number and the distribution of cross-sectional polynomials) is completely independent of the choice of the beam finite element to be used along the beam axis. In this work, 1D Lagrange elements with four nodes (B4) are adopted, i.e. a cubic approximation along the y-axis is assumed.

The stiffness and mass matrices of the elements are obtained hereinafter through the principle of virtual displacements, which in the case of undamped free vibration states

$$\delta L_{int} = \int_V (\delta \boldsymbol{\epsilon}_p^T \boldsymbol{\sigma}_p + \delta \boldsymbol{\epsilon}_n^T \boldsymbol{\sigma}_n) dV = -\delta L_{ine} \tag{13}$$

where L_{int} stands for the strain energy and L_{ine} is the work of the inertial loadings. δ stands for the virtual variation. The virtual variation of the strain energy δL_{int} is rewritten using Eqs. (3), (6), (8) and (11) to give

$$\delta L_{int} = \delta \mathbf{q}_{\tau i}^T \mathbf{K}^{ij\tau s} \mathbf{q}_{sj} \tag{14}$$

$\mathbf{K}^{ij\tau s}$ is the stiffness matrix in the form of the fundamental nucleus. In a compact notation, it can be written as

$$\begin{aligned} \boldsymbol{K}^{ij\tau s} \;=\; & I_l^{\;ij} \triangleleft \left(\boldsymbol{D}_{np}^T F_\tau \, \boldsymbol{I}\right) \Big[\tilde{\boldsymbol{C}}_{np} \left(\boldsymbol{D}_p F_s \, \boldsymbol{I}\right) \,+\, \tilde{\boldsymbol{C}}_{nn} \left(\boldsymbol{D}_{np} F_s \, \boldsymbol{I}\right) \Big] \,+ \\ & \left(\boldsymbol{D}_p^T F_\tau \, \boldsymbol{I}\right) \Big[\tilde{\boldsymbol{C}}_{pp} \left(\boldsymbol{D}_p F_s \, \boldsymbol{I}\right) \,+\, \tilde{\boldsymbol{C}}_{pn} \left(\boldsymbol{D}_{np} F_s \, \boldsymbol{I}\right) \Big] \triangleright_\Omega \,+ \\ & I_l^{\;ij,_y} \triangleleft \Big[\left(\boldsymbol{D}_{np}^T F_\tau \, \boldsymbol{I}\right) \tilde{\boldsymbol{C}}_{nn} \,+\, \left(\boldsymbol{D}_p^T F_\tau \, \boldsymbol{I}\right) \tilde{\boldsymbol{C}}_{pn} \Big] F_s \triangleright_\Omega \boldsymbol{I}_{\Omega\, y} \,+ \\ & I_l^{\;i,_y j} \, \boldsymbol{I}_{\Omega\, y} \triangleleft F_\tau \Big[\tilde{\boldsymbol{C}}_{np} \left(\boldsymbol{D}_p F_s \, \boldsymbol{I}\right) \,+\, \tilde{\boldsymbol{C}}_{nn} \left(\boldsymbol{D}_{np} F_s \, \boldsymbol{I}\right) \Big] \triangleright_\Omega \,+ \\ & I_l^{\;i,_y j,_y} \, \boldsymbol{I}_{\Omega\, y} \triangleleft F_\tau \, \tilde{\boldsymbol{C}}_{nn} F_s \triangleright_\Omega \boldsymbol{I}_{\Omega\, y} \end{aligned} \tag{15}$$

where

$$\boldsymbol{I}_{\Omega\, y} \;=\; \begin{bmatrix} 0 & 1 & 0 \\ 1 & 0 & 0 \\ 0 & 0 & 1 \end{bmatrix} \qquad\qquad \triangleleft \ldots \triangleright_\Omega \;=\; \int_\Omega \ldots \, d\Omega \tag{16}$$

$$\left(I_l^{\;ij}, \, I_l^{\;ij,_y}, \, I_l^{\;i,_y j}, \, I_l^{\;i,_y j,_y}\right) \;=\; \int_l \Big(N_i \, N_j, \; N_i \, N_{j,_y}, \; N_{i,_y} \, N_j, \; N_{i,_y} \, N_{j,_y} \Big) \, dy \tag{17}$$

The nine components of the fundamental nucleus of the matrix $\boldsymbol{K}^{ij\tau s}$ can be found in explicit form in [39].

The virtual variation of the work of the inertial loadings is

$$\delta L_{ine} = \int_V \rho \delta \mathbf{u}^T \ddot{\mathbf{u}} dV \tag{18}$$

where ρ is the density of the material and $\ddot{\mathbf{u}}$ is the acceleration vector. Equation (18) is rewritten using

Eqs. (8) and (11):

$$\delta L_{ine} = \delta \mathbf{q}_{\tau i}^T \mathbf{M}^{ij\tau s} \ddot{\mathbf{q}}_{sj} \tag{19}$$

where $\boldsymbol{M}^{ij\tau s}$ is the fundamental nucleus of the mass matrix. In compact form it can be written as:

$$\boldsymbol{M}^{ij\tau s} = I_l^{ij} \lhd \left(F_\tau \rho \boldsymbol{I} F_s \right) \rhd \tag{20}$$

It should be noted that both $\boldsymbol{K}^{ij\tau s}$ and $\boldsymbol{M}^{ij\tau s}$ do not depend either on the expansion order or on the choice of the F_τ expansion polynomials. These are the key points of CUF that makes possible the straightforward formulation of any-order multiple class theories. In fact, the fundamental nuclei have to be expanded according to the indexes τ and s in order to obtain the elemental FE matrices of the arbitrary-order beam theory. The elemental matrices can then be assembled in the classical way of FEM by using beam nodes indexes i and j.

Once the global FE matrices are assembled, the undamped dynamic problem can be written as follows:

$$\mathbf{M}\ddot{\mathbf{q}} + \mathbf{K}\mathbf{q} = 0 \tag{21}$$

Introducing harmonic solutions, it is possible to compute the natural frequencies, ω_k, by solving a classical eigenvalue problem,

$$(-\omega_k^2 \mathbf{M} + \mathbf{K})\mathbf{q}_k = 0 \tag{22}$$

where $\mathbf{q}_k$ is the k^{th} eigenvector.

3 Results and Discussion

3.1 Validation

Six-layer plate

To validate the present methodology, the free vibration analysis of a six-layer plate with a symmetric stacking sequence was carried out first. The plies are of equal thickness and they are made of orthotropic material with Young modulus along the fibre direction equal to $E_L = 98$ GPa, Young modulus along a transverse direction $E_T = 7.90$ GPa, shear modulus $G_{LT} = 5.60$ GPa, Poisson ratio $\nu = 0.28$ and density $\rho = 1520$ Kg/m^3. The length, the width and the total thickness of the structure are equal to 305, 76.2 and 0.804 mm, respectively.

The proposed composite plate is modelled by means of the present beam theory and, in particular, six quadratic (L9) Lagrange polynomials are used to formulate the theory kinematics. In other words, one L9 polynomial set is used to approximate each layer on the beam cross-section. On the contrary, ten

Table 1: Natural frequencies [Hz] of the six-layer plate for various stacking sequences.

	Present 6L9			Exp. [48]			2D FE [48]		
	B_1	B_2	T_1	B_1	B_2	T_1	B_1	B_2	T_1
$[0_2/90]_s$	11.23	70.340	39.684	11.	70.5	42.0	11.1	69.5	39.5
$[15_2/0]_s$	8.941	62.848	42.946	9.4	66.2	45.8	8.9	62.7	42.9
$[30_2/0]_s$	6.315	37.525	57.778	6.6	40.0	59.1	6.3	37.3	56.9
$[45_2/0]_s$	4.891	30.258	50.906	4.8	29.8	51.3	4.9	30.1	49.4
$[60_2/0]_s$	4.185	26.126	42.555	4.3	27.1	47.7	4.2	26.1	41.7
$[75_2/0]_s$	3.879	24.288	36.879	3.8	25.1	38.9	3.9	24.3	36.7
$[90_2/0]_s$	3.804	23.839	35.103	3.7	24.3	38.2	3.8	23.9	35.1

B: bending mode; T: torsional mode.

4-node (B4) elements are adopted along the beam axis. The total number of the degrees of freedom of the proposed beam model of the composite plate is 3627. Table 1 quotes both bending (B) and torsional (T) natural frequencies of the plate for various stacking sequences and it compares the computed results with the experimental evidences and the finite element solutions provided in [48]. The comparisons reveal good agreement with the reference solutions.

CUS box beam

In the second validation test case, the same composite box beam as analyzed in [49] is considered. The cantilever beam is prismatic with length $L = 762$ mm, width $b = 24.21$ mm and height $h = 13.46$ mm. Each wall of the box has a total thickness equal to $t = 0.762$ mm and it is made of six equal layers. In this example, a CUS (Circumferentially Uniform Stiffness) stacking sequence $[\theta]_6$ is addressed. Each layer of the structure is made of an orthotopic material, whose density and mechanical properties along the fibre (L) and transverse (T) directions are: $\rho = 1601$ Kg/m^3, $E_L = 142$ GPa, $E_T = 9.8$ GPa, $G_{LT} = 6.0$ GPa, $G_{TT} = 4.83$ GPa, $\nu_{LT} = 0.42$, $\nu_{TT} = 0.5$. The proposed CUF beam structural model makes use of four L9 polynomials (one for each wall of the box) to approximate the cross-section kinematics, whereas ten 4-node beam finite elements are utilized along the longitudinal axis.

Figure 4-a shows, in a graphical form, the natural frequencies related to some important vertical (VB) and horizontal (HB) bending mode shapes for various angles θ. Also, the figure compares the results by the present model, which is referred to as 4L9, with the analytical solution provided by Armanios and Badir [49]. Figure 4-b shows the influence of θ on the natural frequencies related to twist-extension modes. According to the notation used in [49], S modes correspond to twist-extension modes which are dominated by the torsion (note that, when $\theta = 0$ deg, the mode S is purely torsional). On the contrary, the twist-extension modes which are dominated by extensional deformations are denotes to as P in Fig. 4-b.

From the results given, it should be clear that ply angles up to 60 deg have a significant influence on the natural bending frequencies and the proposed beam model is in good agreement with the analytical

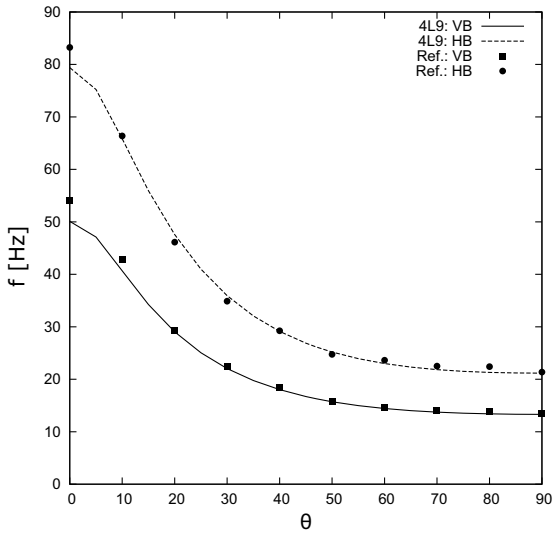

(a) Vertical (VB) and Horizontal (HB) bending modes by 4L9 and solution from [49]

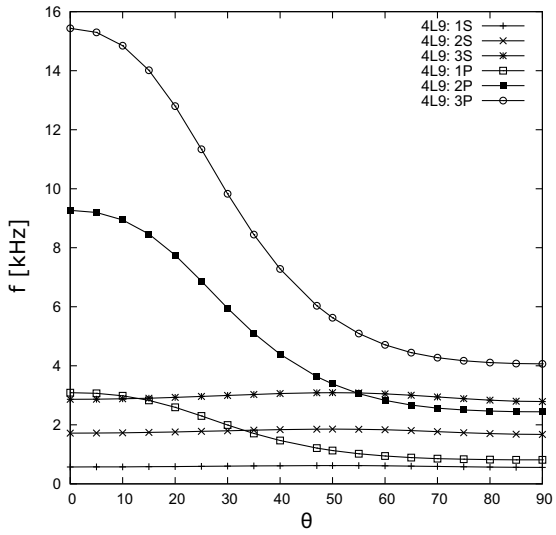

(b) Extension-twist coupled modes

Figure 4: Natural frequencies vs. ply angle for the CUS box beam with $[\theta]_6$ lamination scheme.

Lay-up	Flanges		Webs	
	Top	Bottom	Left	Right
Case 1	θ	θ	θ	θ
Case 2	θ	θ	0	0
Case 3	0	0	θ	θ
Case 4*	θ	$k_1\theta$	$k_1k_2\theta$	$k_1k_2k_3\theta$

*: $k_1 = -1$, $k_2 = 2$, $k_3 = -1$

Table 2: The different lamination sequences of the single-layer box beam.

reference solutions. Moreover, unlike S modes, the twist-extension modes dominated by extension (modes P) are significantly affected by θ in the case of the CUS box beam under consideration.

3.2 Tailoring of single-layer box beam

In this section, the vibration tailoring of a composite box structure is discussed. The dimensions of the cross-section (i.e., the width b and the height h) are assumed to be equal as in the previous analysis case. The length-to-height ratio, L/h, is assumed equal to 15 and each wall of the box is made of one single layer of thickness equal to $t = 0.762$ mm. Table 2 shows the different lamination schemes addressed in the following analysis.

The mathematical LE beam models considered in the proposed assessments consist of seven 4-node beam elements along the longitudinal axis. On the other hand, various approximations of the cross-section kinematics are assumed and they are depicted in Fig. 5, where each rectangle represents one L9 polynomials set. It is, thus, clear that two 16L9 and one 24L9 models are considered.

For validation purpose, Table 3 quotes the important natural frequencies by the proposed LE models and a solid model by MSC.Nastran built with 8-node hexahedral 3D finite elements. In the table, the first two bending modes in the plane yz (B^{yz}), the first bending mode in the plane xy (B^{xy}), the first

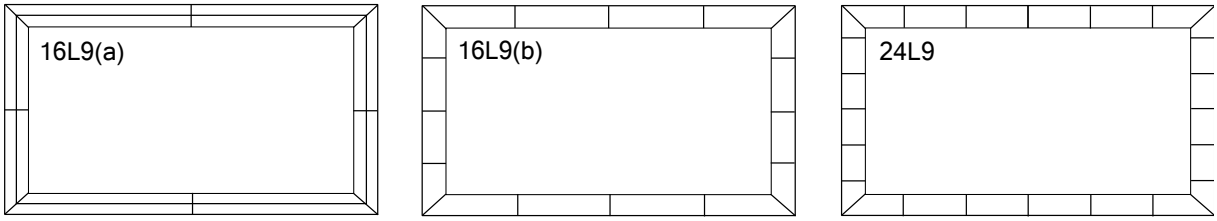

Figure 5: L9 approximations of beam kinematics of the single-layer box beam.

		16L9(a)	16L9(b)	24L9	MSC.Nastan
	DOFs	5280	6336	7920	360000
Case 1	$1B^{yz}$	$232.02^{(-0.15)}$	$233.28^{(0.38)}$	$233.66^{(0.55)}$	232.38
	$1B^{xy}$	$373.11^{(0.83)}$	$371.69^{(0.45)}$	$372.49^{(0.67)}$	370.01
	$2B^{yz}$	$1381.9^{(0.70)}$	$1379.1^{(0.50)}$	$1384.2^{(0.87)}$	1372.2
	1T	$2499.3^{(20.9)}$	$2061.3^{(-0.24)}$	$2079.3^{(0.62)}$	2066.4
	1S	$3677.4^{(-0.09)}$	$2932.1^{(-20.3)}$	$3040.8^{(-17.3)}$	3680.9
Case 3	$1B^{yz}$	$610.78^{(1.03)}$	$605.73^{(0.20)}$	$607.20^{(0.44)}$	604.52
	$1B^{xy}$	$711.23^{(0.24)}$	$710.05^{(0.07)}$	$710.31^{(0.11)}$	709.49
	$2B^{yz}$	$2784.9^{(11.4)}$	$2510.7^{(0.47)}$	$2580.2^{(3.25)}$	2498.9
	1T	$1816.1^{(-1.60)}$	$1700.6^{(-7.86)}$	$1743.5^{(-5.54)}$	1845.8
	1S	$3020.3^{(-3.13)}$	$2767.8^{(-11.2)}$	$2818.1^{(-9.61)}$	3117.9

Table 3: Comparisons of frequencies for Case 1 and 3 with $\theta = 45$ deg.

torsional mode (T) and the first shell-like mode (S) are reported. It should be underlined that shell-like modes are those vibration modes that are dominated by cross-sectional deformations. The results listed in the table are related to the first and third lamination sequences of Table 2 with $\theta = 45\,\text{deg}$. For the sake of clarity, the number of degrees of freedom (DOFs) is given and the percentage differences between the present beam theories and the 3D FEM model are reported in brackets.

From the analysis conducted, it is clear that, in the case of bending frequencies (B), the maximum difference (11.4%) with respect to the solid reference model occurs for the 16L9(a) beam model. For the torsional frequency, this difference increases up to 20.9% for the lamination scheme Case 1. Contrarily, the 16L9(b) and 24L9 beam theories predict lower shell type frequencies than the 3D FEM model. The differences between the two 16L9 models are due to the occurrence of significant in-plane deformations (also present in the case of bending and torsional mode shapes), which can be accurately predicted by using more than two quadratic polynomial sets along the length of the walls. However, the 16L9(a) model may be used for the modelling of stiffer cross-sections. To highlight the significant transversal deformations involved in the proposed analysis, Fig. 6 shows the torsional (T) and shell type (S) mode shapes by the 16L9(b) model and Case 1.

The vibration tailoring of the composite box is discussed in the following. In the remaining analyses, the 16L9(b) model (see Fig. 5) is employed. For the different lamination schemes (Case 1 to 4, see Table 2), Fig. 7 shows the variations of the natural frequencies versus θ. In particular, the graphs are related to the first bending modes (Fig. 7a-c), the mode dominated by the torsion (Fig. 7d) and the first

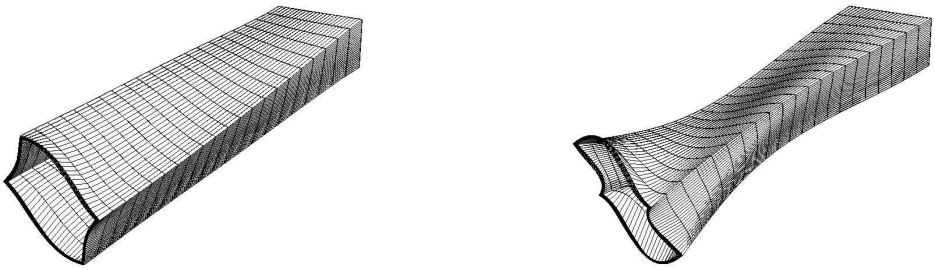

(a) Torsional mode (1T) (b) Shell-like mode (1S)

Figure 6: Important mode shapes of the single-layer box. Case 1 ($\theta = 45$ deg), 16L9(b) beam model.

Mode	$1B^{yz}$	$1B^{xy}$	$2B^{yz}$	1T	1S
	623.07	979.60	2258.8	1573.2	2398.3

Table 4: Natural frequencies [Hz] of the single-layer box beam and $\theta = 0$ deg. 16L9(b) beam model.

mode that involves significant cross-sectional deformations (Fig. 7e). The natural frequencies (f) are given in the non-dimensional form $f/f_{\theta=0}$, where $f_{\theta=0}$ is the corresponding value for $\theta = 0$. For the sake of completeness, the important frequencies for the composite box and $\theta = 0$ are given in Table 4.

The results provided reveal that:

- With the exception of Case 4 and $\theta = 90$ deg, the bending frequencies $1B^{yz}$ and $1B^{xz}$ decrease monotonically as the fibre angle increases. For both these mode shapes, Case 1 determines the maximum relative variations (about 70%).
- The second bending frequency $2B^{yz}$ increases slightly with angle θ, when the third lamination scheme (Case 3) is adopted. The same phenomenon is not verified in the case of Cases 1, 2 and 4.
- For all the lamination schemes (Cases 1 to 4) and in almost the whole domain, the torsional frequencies increase with respect to the reference value as the fibre angle is increased. The maximum percentage variation (about 44%) occurs for Case 4 and $\theta = 35$ or 70 deg.
- In the case of shell-like vibration mode and Case 1 stacking sequence, the natural frequency sharply increases for values of θ higher than 30 deg.

3.3 Tailoring of two-layer box beam

In this analysis case, the box beam of the previous analysis case is considered and each wall is now made of two layers of equal thickness, t=0.381 mm. The lamination scheme of the inner layers is $[\theta]$ whereas for the outer layers is $[k\theta]$, where k is a constant value equal to -1, 0 and 2. The adopted CUF LE model utilized 32L9 on the beam cross-section and seven 4-node beam elements along the longitudinal direction.

Figure 8 shows the frequency variations [Hz] for the three values of the parameter k. The results show that:

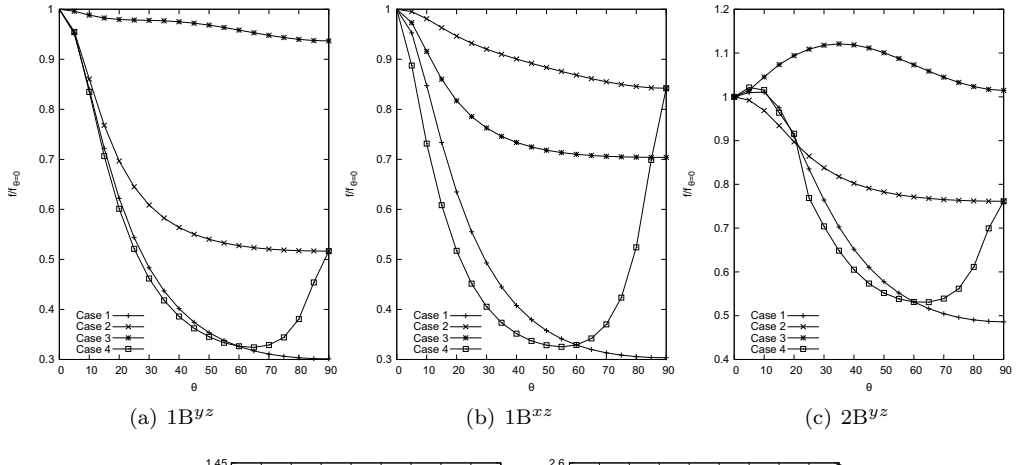

(a) $1B^{yz}$ (b) $1B^{xz}$ (c) $2B^{yz}$

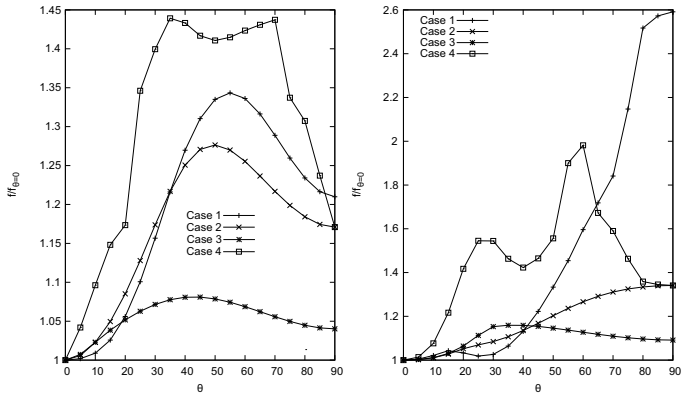

(d) Torsional (e) Shell type

Figure 7: Variations vs θ of the non-dimensional natural frequencies of the single-layer box beam for various lamination schemes. 16L9(b) beam model.

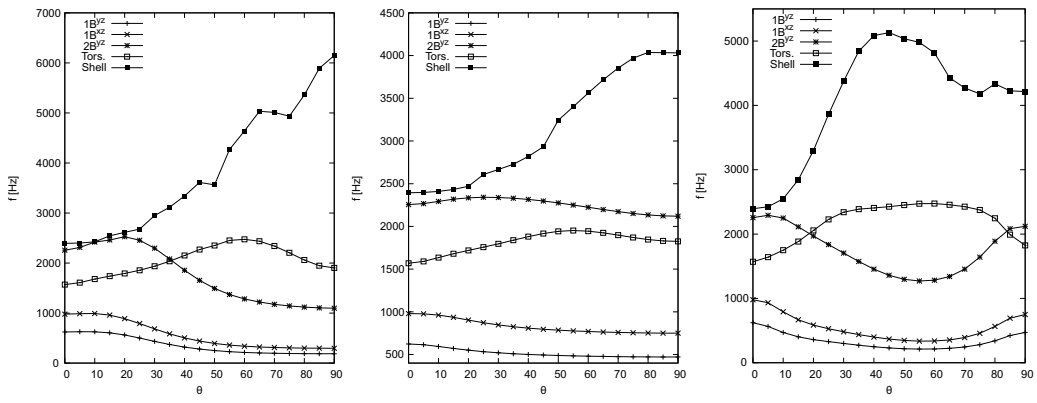

(a) $k = -1$ (b) $k = 0$ (c) $k = 2$

Figure 8: Variations of frequencies [Hz] of the two-layered box beam as functions of θ. 32L9.

Nr. of ribs	$1B^{yz}$	$1B^{xy}$	$2B^{yz}$	1T	1S
1	411.88	647.08	2347.7	2388.8	3134.6
2	410.74	644.73	2321.5	2937.8	3534.1
3	408.50	640.41	2325.1	3204.3	3940.0

Table 5: Frequency [Hz] of the two-layered box beam with one, two and three ribs. θ=30 and k=-1.

- For k =-1, the increasing of the fibre angle entails the decreasing of the bending frequencies $1B^{yz}$ and $1B^{xz}$. In fact, for high values of θ, the bending stiffness of the structure is lowered since the fibres are oriented circumferentially. For the same reason, the shell-type frequency increases as θ rises. On the other hand, the frequencies related to $2B^{yz}$ and the torsional mode reach their maximum at θ=20 and 60 deg, respectively.

- The second configuration with k =0 leads to a slighter decreasing rate of the bending frequencies $1B^{yz}$ and $1B^{xz}$ with respect to the previous case. The torsional natural frequency is lower than the second flexural one $2B^{yz}$ within the whole range of interest. Although the maximum shell type frequency is lower than that one of the previous lamination scheme, it still increases as the fibre angle increases;

- In the case k =2, the three bending frequencies $1B^{yz}$, $1B^{xz}$ and $2B^{yz}$ reach their minimum values for θ = 55 deg. For approximately the same fibre angle, both torsional and shell type frequencies reach their maximum values.

3.4 Effects of ribs and cut-offs

The effects of transverse reinforcements on the free vibration characteristics of the two-layered box beam of the previous example are evaluated. For this analysis case, the k parameter of Section 3.3 is assumed to be equal to -1 and the 16L9(a) beam model of Fig.5 is adopted. The structural configurations considered are reinforced with one, two and three equidistant ribs. Each metallic reinforcement is modelled with one single B4 beam element along its thickness (0.762 mm) and 17L9 are adopted on the rib cross-section. For further details on the modelling of reinforced-shell structures by LE the reader is referred to [41]. The material adopted for the ribs is an aluminium alloy and has the following mechanical properties: E=75 Gpa, ν=0.33 and ρ=2700 kg/m^3.

Table 5 lists the natural frequencies for the single- to the three-rib configurations assuming θ=30. As expected, the most significant variations concern the frequencies related to the mode shapes dominated by the torsional and shell type deformations. The relative increments of these frequencies between the structures with one and three ribs are 34.1% and 25.7%. In Fig.9, the variations of the bending, torsional and shell type frequencies with the fibre angle are shown.

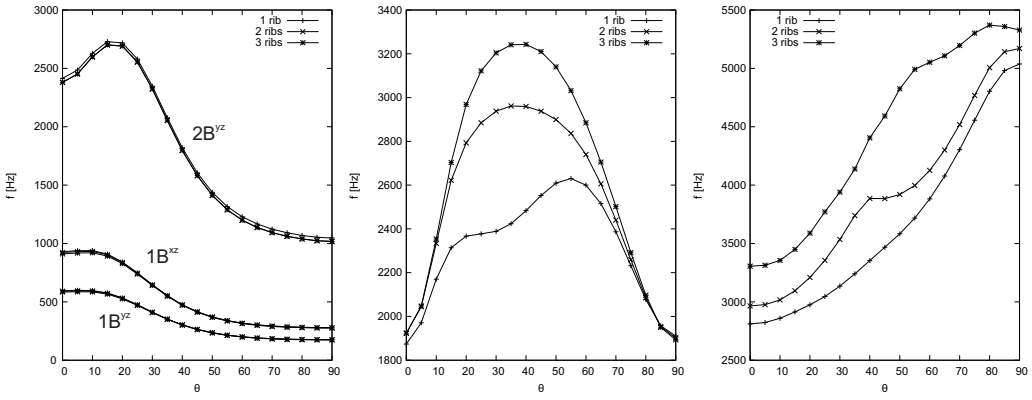

(a) Bending (b) 1st Torsional (c) 1st Shell-type

Figure 9: Variations of frequencies [Hz] of the two-layered box beam with one, two and three ribs. 16L9(a).

The following conclusions stem from the analysis:

- The bending frequencies are not significantly affected by the number of ribs.
- As far as the torsional frequency is concerned, significant differences between the three configurations are evident when $15< \theta <70$ deg.
- The first shell-type frequency increases as the ply angle rises. As expected, the highest values of the shell-type natural frequency are related to the structure with three ribs.

By referring to the composite box beam with three ribs, the effects of a cut-off on the frequencies are evaluated in the final analysis case. The opening is located in the middle bay and it has a width (along the x-axis) and a length (along the y-axis) equal to b/2 and 2L/9, respectively. The related results are shown in Fig. 10, where the important frequencies are graphically shown versus the fibre orientation angle. The analysis suggests that:

- The cut-off affects the variations of the bending frequencies only partially.
- On the other hand, a significant decreasing of the torsional stiffness of the whole structure is observed as the cut-off is considered. In fact, the difference between the maximum torsional frequency with and without the opening is about 27%.
- Although the shell type modes appear at lower frequencies with respect to those of the case without the cut-off (see Fig. 9c), the eigenvalues increase with the fibre angle.

4 Conclusions

In this paper, refined beam theories have been used to study the free vibration characteristics of laminated thin-walled structures in a *composite tailoring* scenario. Enhanced one-dimensional models have been

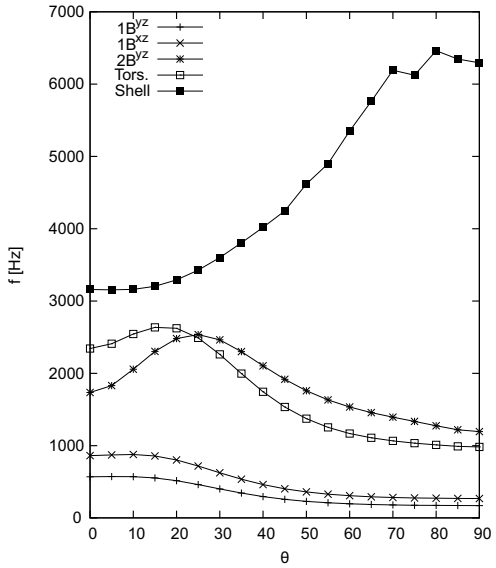

Figure 10: Variations of frequencies [Hz] of the two-layered box beam with three ribs and one cut-off.

conceived using the Carrera Unified Formulation (CUF) and the governing equations have been solved by the finite element method. According to CUF, refined beam theories have been formulated by adopting an LE (Lagrange Expansion) of the primary mechanical unknowns. Thus, higher-order 1D models that are geometrically and physically consistent can be developed in a straightforward manner by only utilizing displacement variables. Moreover, composite box structures including reinforcements and cut-offs can be easily implemented due to the capability of the present methodology to deal with full material anisotropy and component-wise accuracy. Various composite box beams with single- and two-layer laminated walls have been analysed and the attention has been focussed on the parametric study and tailoring of the lamination scheme versus free vibration analysis. Classical and non-classical lamination sequences have been considered, and the variations of the bending, torsional, and shell-type frequencies against fibre orientation angles have been evaluated. Moreover, the effects of transversal reinforcements and cut-offs on the dynamic behaviour have been studied. The provided comparisons have revealed that the 1D-CUF approach yields eventually the same results of the high-fidelity (3D solid) element solutions with a lower computational cost. The efficiency and the accuracy of the proposed LE models, thus, make the proposed formulation a good candidate for the tailoring analysis of composite box structures, eventually to be coupled with optimisation algorithms.

References

[1] P. C. Yang, C. H. Norrish, and Y. Stavsky. Elastic wave propagation in heterogeneous plates. *International Journal of Solid and Structures*, 2(4):665–684, 1996.

[2] J. M. Whitney and C. T. Sun. A higher order theory of extension motion of laminated composite.

Journal of Sound and Vibration, 30(1):85–97, 1973.

[3] J. N. Reddy, C.M. Wang, and K.H. Lee. Relationship between bending solution of classical and shear deformation beam theories. *International Journal of Solids and Structures*, 34(26):3373–3384, 1997.

[4] G. Shi. A new simple third order shear deformation theory of plates. *International Journal of Solids and Structures*, 44:4394–4417, 2007.

[5] R. Sahoo and B.N. Singh. A new inverse hyperbolic zigzag theory for the static analysis of laminated composite and sandwich plates. *Composite Structures*, 105:385–397, 2013.

[6] E. Carrera. The effects of shear deformation and curvature on buckling and vibration of cross-ply laminated composite shells. *Journal of Sound and Vibration*, 150(3):405–433, 1991.

[7] G. Shi and K. Y. Lam. Finite element vibration analysis of composite beams based on higher-order beam theory. *Journal of Sound and Vibration*, 219(4):707–721, 1999.

[8] A. Ozutok and E. Madenci. Free vibration analysis of cross ply laminated composite beam by mixed finite element formulation. *Int.J. Str. Stab. Dyn.*, 13:125–0056, 2013.

[9] M. K. Rao, Y. M. Desai, and M. R. Chitnis. Free vibrations of laminated beams using mixed theory. *Composite Structures*, 52:149–160, 2001.

[10] J. R. Banerjee, H. Su, and C. Jayatunga. A dynamic stiffness element for free vibration analysis of composite beams and its application to aircraft wings. *Computers and Structures*, 86:573–579, 2008.

[11] S.G. Lekhnitskii. *Anisotropic Plates*. Bordon and Breach, New York, 2nd edition, 1968. Translated from the second Russian Edited by S.W. Tsai and T. Cheron.

[12] D.H. Robbin and J.N. Reddy. Modelling of thick composites using a layerwise laminate theory. *International Journal for Numerical Methods in Engineering*, 36(4):655–677, 1993.

[13] R.P. Shimpi and A.V. Ainapure. A beam finite element based on layerwise trigonometric shear deformation theory. *Composite Structures*, 53:153–162, 2007.

[14] L. Dinghe, Y. Liu, and X. Zhang. A layerwise or solid element method of the linear static and free vibration analysis for the composite sandwich plates. *Composites Part B: Engineering*, 52:187–198, 2013.

[15] S. Kapuria and G.G.S. Achary. Nonlinear coupled zigzag theory for buckling of hybrid piezoelectric plates. *Composite Structures*, 74(3):253–264, 2006.

[16] S. Kapuria and S.D. Kulkarni. An improved discrete Kirchhoff quadrilateral element based on third-order zigzag theory for static analysis of composite and sandwich plates. *International Journal for Numerical Methods in Engineering*, 69(9):1948–1981, 2007.

[17] A. Chattopadhyay. *Development of a Composite Tailoring Procedure for Airplane Wing.* NASA CR-199081, 1997.

[18] V. Z. Vlasov. *Thin-walled elastic beams.* National Science Foundation, Washington, 1961.

[19] M.G. Gunay and T. Timarci. Free vibration of composite box-beams by ANSYS. In *International Scientific Conference*, Gabrovo, 16-17 November 2012.

[20] S. Durmaz. Free vibration of an anisotropic thin-walled box beam under bending-torsion coupling. In *Proceedings of the 3rd International Conference on Integrity, Reliability and Failure*, Porto, Portugal, July 2009.

[21] C. Kim and S. R. White. Thick-walled composite beam theory including 3-D elastic effects and torsional warping. *International Journal of Solids and Structures*, 34(31-32):4237–4259, 1997.

[22] C. Kim and S. R. White. Analysis of thick hollow composite beams under general loadings. *Composite Structures*, 34:263–277, 1996.

[23] D. S. Dancila and E. A. Armanios. The influence of coupling on the free vibration of anisotropic thin-walled closed-section beams. *Internationl Journal of Solids and Structures*, 35(23):3105–3119, 1998.

[24] V. V. Volovoi and D. H. Hodges. Theory of anisotropic thin-walled beams. *Journal of Applied Mechanics*, 67:453–459, 2000.

[25] V. V. Volovoi, D. H. Hodges, C. E. S. Cesnik, and B. Popescu. Assessment of beam modelling methods for rotor blade applications. *Mathematical and Computer Modelling*, 33(10-11):1099–1112, 2001.

[26] W. Yu, D. H. Hodges, V. V. Volovoi, and C. E. S. Cesnik. On Timoshenko-like modeling of initially curved and twisted composite beams. *International Journal of Solids and Structures*, 39:5101–5121, 2002.

[27] W. Yu, D. H. Hodges, V. V. Volovoi, and E. D. Fuchs. A generalized Vlasov theory for composite beams. *Thin-Walled Structures*, 43:1493–1511, 2005.

[28] Y. Wu, Y. Lai, X. Zhang, and Y. Zhu. A finite beam element for analyzing shear lag and shear deformation effects in composite-laminated box girders. *Computers and Structures*, 82:763–771, 2004.

[29] T. P. Vo and J. Lee. Free vibration of thin-walled composite box beam. *Composite Structures*, 84:11–20, 2008.

[30] T. P. Vo and J. Lee. Flexural-torsional behavior of thin-walled composite box beams using shear-deformable beam theory. *Engineering Structures*, 30:1958–1968, 2008.

[31] Z. Qin and L. Librescu. On a shear-deformable theory of anisotropic thin-walled beams: further contribution and validations. *Composite Structures*, 56:345–358, 2002.

[32] F. Shadmehri, H. Haddadpour, and M. A. Kouchakdeh. Flexural-torsional behavior thin walled composite beams with closed cross-section. *Thin-Walled Structures*, 45:699–705, 2007.

[33] P. P. Friedmann, B. Glaz, and R. Palacios. A moderate deflection composite helicopter rotor blade model with an improved cross-sectional analysis. *International Journal of Solids and Structures*, 46:2186–2200, 2009.

[34] M. Mitra, S. Gopalkrishan, and M. S. Bhat. A new superconvergent thin walled composite beam element for analysis of box beam structure. *International Journal of Solids and Structures*, 41:1491–518, 2004.

[35] A.H. Sheikh and O.T. Thomsen. An efficient beam element for the analysis of laminated composite beams of thin-walled open and closed cross sections. *Composites Science and Technology*, 68:2273–2281, 2008.

[36] E. Carrera. Theories and finite elements for multilayered, anisotropic, composite plates and shells. *Archives of Computational Methods in Engineering*, 56(3):87–140, 2003.

[37] E. Carrera. Theories and finite elements for multilayered plates and shells: a unified compact formulation with numerical assessment and benchmarking. *Archives of Computational Methods in Engineering*, 10(3):216–296, 2003.

[38] E. Carrera, A. Pagani, M. Petrolo, and E. Zappino. Recent developments on refined theories for beams with applications. *Mechanical Engineering Reviews*, 2(2):1–30, 2015.

[39] E. Carrera, M. Filippi, P.K. Mahato, and A. Pagani. Advanced models for free vibration analysis of laminated beams with compact and thin-walled open/closed sections. *Journal of Composite Materials*, 49(17):2085–2101, 2015. DOI: 10.1177/0021998314541570.

[40] E. Carrera, M. Filippi, P.K. Mahato, and A. Pagani. Accurate static response of single- and multi-cell laminated box beams. *Composite Structures*, 136:372–383, 2015. DOI: 10.1177/0021998314541570.

[41] E. Carrera, A. Pagani, and M. Petrolo. Classical, refined and component-wise theories for static analysis of reinforced-shell wing structures. *AIAA Journal*, 51(5):12551268, 2013. DOI: 10.2514/1.J052331.

[42] E. Carrera, A. Pagani, and M. Petrolo. Component-wise method applied to vibration of wing structures. *Journal of Applied Mechanics*, 80:041012, 2013. DOI: 10.1115/1.4007849.

[43] E. Carrera, A. Pagani, and M. Petrolo. Refined 1D finite elements for the analysis of secondary, primary, and complete civil engineering structures. *Journal of Structural Engineering*, 141:04014123/1–14, 2015.

[44] E. Carrera and A. Pagani. Free vibration analysis of civil engineering structures by component-wise models. *Journal of Sound and Vibration*, 333(19):4597–4620, 2014.

[45] E. Carrera and M. Filippi. Variable kinematic one-dimensional finite elements for the analysis of rotors made of composite materials. *Journal of Engineering for Gas Turbines and Power - ASME*, 2014. DOI: 10.1115/1.4027192.

[46] E. Carrera and M. Petrolo. Refined beam elements with only displacement variables and plate/shell capabilities. *Meccanica*, 47(3):537–556, 2012. DOI: 10.1007/s11012-011-9466-5.

[47] K. J. Bathe. *Finite element procedure*. Prentice hall, Upper Saddle River, New Jersey, USA, 1996.

[48] D. W. Jensen and E.F. Crawley. Frequency determination techniques for cantilevered plates with bending-torsion coupling. *AIAA Journal*, 22(3):415–420, 1984. DOI: 10.2514/3.48463.

[49] E.A. Armanios and A.M. Badir. Free vibration analysis of anysotropic thin-wall close-section beams. *AIAA Journal*, 33(10):1905–10, 1995.